Application of the Mössbauer effect to the study of subnanometer harmonic displacements in thin solids

R. N. Shakhmuratov and F. G. Vagizov

Phys. Rev. B **95**, 245429 — Published 26 June 2017

DOI: 10.1103/PhysRevB.95.245429

Application of Mössbauer effect to study subnanometer harmonic displacements in a thin solid

R. N. Shakhmuratov[1,2] and F. G. Vagizov[2]

[1]*Kazan Physical-Technical Institute, Russian Academy of Sciences, 10/7 Sibirsky Trakt, Kazan 420029 Russia*

[2]*Kazan Federal University, 18 Kremlyovskaya Street, Kazan 420008 Russia*

(Dated: June 6, 2017)

Abstract

We measure subnanometer displacements of thin samples vibrated by piezotransducer. Samples contain ^{57}Fe nuclei, which are exposed to 14.4 keV γ-radiation. Vibration produces sidebands from a single absorption line of the sample. The sideband intensities depend on the vibration amplitude and its distribution along the sample. We developed a model of this distribution, which adequately describes the spectra of powder and stainless steel (SS) absorbers. We propose to filter γ-radiation through a small round hole in the lead mask, placed before the absorber. In this case only a small spot of the vibrated absorber is observed. We found for SS foil that nuclei, exposed to γ-radiation in this small spot, vibrate with almost the same amplitudes whose difference does not exceed a few picometers within the irradiated area.

PACS numbers: 42.25.Bs, 42.50.Gy, 42.50.Nn

I. INTRODUCTION

Mössbauer spectroscopy offers a wide range of applications due to very short wavelengths of γ-photons and uniquely large ratios of the nuclear transition energy to the linewidth. Many Mössbauer experiments, valuable from the viewpoint of fundamental interest and applications, were reported since the invention of Mössbauer effect. Among them, we just briefly mention a few. They are gravitational red shift experiments [1–7], novel tests of the general relativity theory [8, 9], detection of fast and tiny sample displacements induced by pulsed-laser heating [10], time differential nuclear resonance spectroscopy of geophysically important materials containing iron under extremely high static pressure and pulsed laser heating, which simulate physical and chemical processes in deep planetary interiors [11]. A rapidly developing field of science, which is known as γ-ray (or hard x-ray) quantum optics based on Mössbauer effect, provides unambiguous test of many concepts and ideas of coherent quantum optics with γ-photons resonantly interacting with ensemble of nuclei. Recent experimental achievements in this domain include electromagnetically induced transparency in a cavity [12], the collective Lamb shift [13], vacuum-assisted generation of atomic coherences [14], single-photon supperradiance in nuclear absorbing multilayer structures [15], slow gamma photon [16], subluminal pulse propagation using nuclear resonances [17], photon shaping [18, 19], and γ-echo [20–22].

The gamma echo is generated if a thin absorber experiences a fast, piston-like displacement equal to a half wavelength of gamma radiation, which is 43 pm for ^{57}Fe. If this displacement is comparable or larger than the wavelength λ of γ-radiation, the gamma-echo exhibits several γ-radiation pulses each time when the absorber displacement reaches the value $\lambda(n + 1/2)$, where n is integer. Therefore we expect that γ-echo could be used, for example, for calibrating the displacement of a scanning tunneling microscope. However, the intensity of γ-echo is quite sensitive to the lateral distribution of the displacements of the absorber along the γ-radiation beam. Therefore, knowledge of the lateral displacement distribution, induced by pizo-transducer, is important. If we could apply γ-radiation for spatial measurements, then Angstrom resolution scale could be achieved. Moreover, the lateral distribution of the displacements of the vibrating absorber is quite important from the viewpoint of high resolution spectroscopy with high- and low-finesse frequency combs [23–25].

In this paper we discuss the application of γ-photons for sub-nanometer spatial measurements with sub-Angstrom resolution for periodical displacements, induced by pizo-transducer. We expect that our results could be applied to calibrate also a step-like displacements, controlled by γ-echo.

We employ 14.4 keV γ-photons, emitted by radioactive ^{57}Co with a wavelength 86 pm. Since we are not able to focus γ-radiation field and direct it to a desirable spot on the sample, we address to the spectral measurements. In our case, transmission spectra of the sample, containing resonant nuclei ^{57}Fe, are proposed to be measured. We expect high depth resolution, while lateral resolution could be controlled by a lead mask with a small aperture, which could be moved along the surface of the sample. We expect that our method could provide controllable and calibrated displacements of the surface with sub-Angstrom resolution, which are produced by piezo-transducer oscillating with high frequency (several MHz), low frequency (several kHz), or experiencing step-like displacement due to the applied step voltage.

In the method, we discuss in this paper, the sample containing resonant nuclei is mechanically vibrated. As a result, along with the main absorption line, a system of satellites appears in the spectrum, spaced apart at distances that are multiples of the vibration frequency. Line intensities of this comb structure are very sensitive to the vibration amplitude, which is extremely small (Angstrom or even smaller). For the stainless steel foil, which is illuminated by γ-radiation transmitted through a small aperture in the lead mask placed before the absorber, we measured displacements of the order of dozens of picometers with the accuracy of a few picometers.

The influence of extremely-small-amplitude mechanical vibrations of the absorbers containing Mössbauer nuclei attracted attention since the invention of Mössbauer spectroscopy. Mössbauer sidebands, produced from a single parent line by absorber vibration, were observed in many different samples [23, 24, 26–34]. However, the intensity of the sidebands has not been yet satisfactory explained [30–32]. There are two models of coherent and incoherent vibrations of nuclei in the absorber [27–32]. Coherent model implies piston-like vibration of the absorber with frequency Ω and phase ψ along the propagation direction of γ quanta. This model predicts the intensity of the n-th sideband proportional to the square of Bessel function $J_n^2(m)$, where $m = 2\pi a_0/\lambda$ is the modulation index, which is proportional to the ratio of the amplitude a_0 of the harmonic displacements $a_z(t) = a_0 \sin(\Omega t + \psi)$ and

the wavelenght λ of γ-photon. The incoherent model, where phase ψ is assumed to be random and distributed with equal probability between 0 and π, was proposed by Abragam [35]. This model is based on the Rayleigh distribution of the nuclear-vibration amplitudes in the absorber, which predicts the sideband intensity proportional to $\exp(-m^2)I_n(m^2)$, where $I_n(m^2)$ is the modified Bessel function. However, both models or their combinations cannot describe perfectly all absorption spectra, which are experimentally observed for samples of different mechanical properties and chemical composition. To support this statement we refer to Chien and Walker who pointed out in Ref. [30] that "while unequivocally measured intensities agree qualitatively with Abragam's sideband theory, no existing theory at present can account quantitatively for the sideband intensities since the amplitude distribution that satisfactorily describes the data are not known at present".

We propose a heuristic distribution of nuclear-vibration amplitudes, which is derived from the Gaussian distribution with appropriate modifications. The vibrations of nuclei in the absorber are supposed to be coherent, i.e., they have the same phase ψ. Our model provides good fitting of experimental spectra. Depending on a parameter of the model σ, the proposed distribution tends to a delta-distribution, inherent to the coherent model if $\sigma \to 0$, or it tends to the Rayleigh distribution inherent to the incoherent model if $\sigma \to 0.72$.

Our model allows to determine from experimental data the amplitude of subnanometer harmonic displacements of the absorber with an accuracy of less than half Angstrom. The method consists of two steps. First, we apply our heuristic distribution to fit the model to experimental spectra. This fitting gives the parameter σ, which specifies the appropriate distribution of the displacements irrespective to their location in the sample. Second, we construct an actual distribution of the vibration amplitudes across the surface of the absorber, which is consistent with our heuristic distribution.

Two absorbers are experimentally studied, i.e., $K_4Fe(CN)_6 \cdot 3H_2O$ powder enriched by ^{57}Fe and stainless steel (SS) foil with natural abundance of ^{57}Fe. For powder, the distribution of the powder-grain displacements, obtained from the spectrum fitting, is close to the continuous uniform distribution with wide scattering of the vibration amplitudes, which is very different from the Rayleigh distribution. For SS foil we found that the displacement distribution along the surface of a thin foil is close to the narrow, bell-shape distribution. Physical interpretation of these results is discussed.

For SS foil we experimentally verified our conclusions placing a lead mask just in the

front of the absorber. We made an aperture in the lead mask and compared the observed Mössbauer spectra with our theoretical predictions. We observed a change of Mössbauer spectra with decrease of the size of the aperture, supporting firmly our model. We moved the narrowest aperture of the lead mask along the surface of the vibrated SS foil and could detect the change of the vibration amplitude along the SS foil, which is deduced from the spectrum analysis. In addition to a scientific value of our model giving an explanation of physical properties of the Mössbauer sidebands, produced by the absorber vibration, we expect that our findings could give an impetus to the development of the method measuring extra-small displacements with an accuracy of less than half Angstrom.

II. COHERENT AND INCOHERENT MODELS OF THE MECHANICAL VIBRATION OF THE ABSORBER

The propagation of γ radiation through a resonant Mössbauer medium vibrating with frequency Ω may be treated classically [36]. In this approach the radiation field from the source nucleus after passing through a small diaphragm is approximated as a plane wave propagating along the direction **z**. In the coordinate system rigidly bounded to the absorbing sample, the field, seen by the absorber nuclei, is described by expression

$$E_S(t-t_0) \propto \theta(t-t_0)e^{-(i\omega_S+\Gamma_0/2)(t-t_0)+ikz+i\varphi(t)}, \tag{1}$$

where ω_S and k are the carrier frequency and the wave number of the radiation field, $1/\Gamma_0$ is the lifetime of the excited state of the emitting source nucleus, t_0 is the instant of time when the excited state is formed, $\Theta(t-t_0)$ is the Heaviside step-function, $\varphi(t) = 2\pi a_z(t)/\lambda = m\sin(\Omega t+\psi)$ is a time dependent phase of the field due to a piston-like periodical displacement $a_z(t)$ of the absorber with respect to the source, ψ is the vibration phase, and λ is the radiation wavelength.

The radiation field (1) can be expressed as polychromatic radiation with a set of spectral lines $\omega_S - n\Omega$ ($n = 0, \pm1, \pm2, ...$), i.e.,

$$E_S(t-t_0) = E_C(t-t_0)e^{-i\omega_S(t-t_0)+ikz}\sum_{n=-\infty}^{+\infty} J_n(m)e^{in(\Omega t+\psi)}, \tag{2}$$

where $E_C(t-t_0) = E_0\theta(t-t_0)e^{-\Gamma_0(t-t_0)/2}$ is the common part of the field components, E_0 is the field amplitude, and $J_n(a)$ is the Bessel function of the nth order. The Fourier transform

of this field has a frequency comb structure

$$E_S(\omega) = E_0 \sum_{n=-\infty}^{+\infty} \frac{J_n(m) e^{in(\Omega t_0 + \psi)}}{\Gamma_0/2 + i(\omega_S - n\Omega - \omega)}, \tag{3}$$

where for shortening of notations the exponential factor with ikz is omitted. From this expression, it follows that the vibrating absorber 'sees' the incident radiation as an equidistant frequency comb with spectral components $\omega_S - n\Omega$ whose amplitudes are proportional to the Bessel functions $J_n(m)$.

The Fourier transform of the radiation field is changed at the exit of the resonant absorber as (see [18, 19, 24, 36])

$$E_{\rm out}(\omega) = E_0 \sum_{n=-\infty}^{+\infty} \frac{J_n(m) \exp\left[in(\Omega t_0 + \psi) - \frac{b}{\Gamma_A/2 + i(\omega_A - \omega)}\right]}{\Gamma_0/2 + i(\omega_S - n\Omega - \omega)}, \tag{4}$$

where ω_A and Γ_A are the frequency and linewidth of the absorber, $b = T_A\Gamma_0/4$ is the parameter depending on the effective thickness of the absorber $T_A = f_A n_A \sigma_A$, f_A is the Debye-Waller factor, n_A is the number of ^{57}Fe nuclei per unit area of the absorber, and σ_A is the resonance absorption cross section. The source linewidth Γ_S can be different from Γ_0 due to the contribution of the environment of the emitting nucleus in the source. In this case Γ_0 can be simply substituted by Γ_S in Eq. (4). Here, nonresonant absorption is disregarded. Recoil processes in nuclear emission are not taken into account assuming that recoilless fraction of the source emission (Debye-Waller factor) is $f_A = 1$. These processes can be easily taken into account in experimental data analysis.

Time dependence of the amplitude of the output radiation field is found by inverse Fourier transformation

$$E_{\rm out}(t - t_0) = \frac{1}{2\pi} \int_{-\infty}^{+\infty} E_{\rm out}(\omega) e^{-i\omega(t - t_0)} d\omega. \tag{5}$$

In the laboratory reference frame this field is transformed as

$$E_{\rm lab}(t - t_0) = E_{\rm out}(t - t_0) e^{-i\varphi(t)}. \tag{6}$$

Since the fields $E_{\rm lab}(t - t_0)$ and $E_{\rm out}(t - t_0)$ differ only in the phase $\varphi(t)$, the intensity seen by the detector, $I_{\rm lab}(t - t_0) = |E_{\rm lab}(t - t_0)|^2$, coincides with the intensity of the radiation field in the vibrated reference frame $I_{\rm out}(t - t_0) = |E_{\rm out}(t - t_0)|^2$, i.e.,

$$I_{\rm lab}(t - t_0) = I_{\rm out}(t - t_0). \tag{7}$$

This condition is valid if we use the detection scheme, which is not sensitive to the spectral content of the radiation field filtered by the vibrated absorber. If the second absorber (spectrum analyzer) is placed between the vibrated source and detector, then another description of the radiation intensity is necessary [33, 34].

Since we don't use a second single line resonance filter analyzing the spectra of γ radiation emerging from the vibrated absorber, the intensity of the field, registered by a detector, can be described by expression

$$I_{\rm out}(t-t_0)=\frac{1}{(2\pi)^2}\int_{-\infty}^{+\infty}d\omega_1\int_{-\infty}^{+\infty}d\omega_2 E_{\rm out}(\omega_1)E^*_{\rm out}(\omega_2)e^{i(\omega_2-\omega_1)(t-t_0)}. \tag{8}$$

Thus, in our case the radiation intensity at the exit of the vibrating absorber is the same if the source is vibrated instead of absorber.

Frequency-domain Mössbauer spectrum is measured by counting the number of photons, detected within long time windows of the same duration for all resonant detunings, which are varied by changing the value of a velocity of the Mössbauer drive moving the source. Time windows are not synchronized with the mechanical vibration and their duration $T_{\rm w}$ is much longer than the oscillation period $T_{\rm osc}=2\pi/\Omega$. Since the emission time of γ-photons is random, the observed radiation intensity is averaged over t_0

$$\langle I_{\rm out}(t-t_0)\rangle_{t_0}\propto\frac{1}{T_{\rm w}}\int_{-T_{\rm w}/2}^{+T_{\rm w}/2}I_{\rm out}(t-t_0)dt_0, \tag{9}$$

where for simplicity we assume that $T_{\rm w}\to\infty$. Then, the observed number of photon counts, which is proportional to the intensity, i.e., $N_{\rm out}(\Delta)=\langle I_{\rm out}(t-t_0)\rangle_{t_0}$, varies with the change of the resonant detuning $\Delta=\omega_A-\omega_S$ as

$$N_{\rm out}(\Delta)=\sum_{n=-\infty}^{+\infty}J_n^2(m)B_n(\Delta), \tag{10}$$

where

$$B_n(\Delta)=\frac{\Gamma_S}{2\pi}\int_{-\infty}^{+\infty}\frac{e^{-\frac{b\Gamma_A}{(\Gamma_A/2)^2+(\Delta+n\Omega-\omega)^2}}}{(\Gamma_S/2)^2+\omega^2}d\omega. \tag{11}$$

A. Coherent model

If all the nuclei in the absorber vibrate with the same phase and amplitude, then a single parent line is transformed into a set of spectral lines $\omega_S\pm n\Omega$ $(n=0,1,2,...)$ spaced apart at

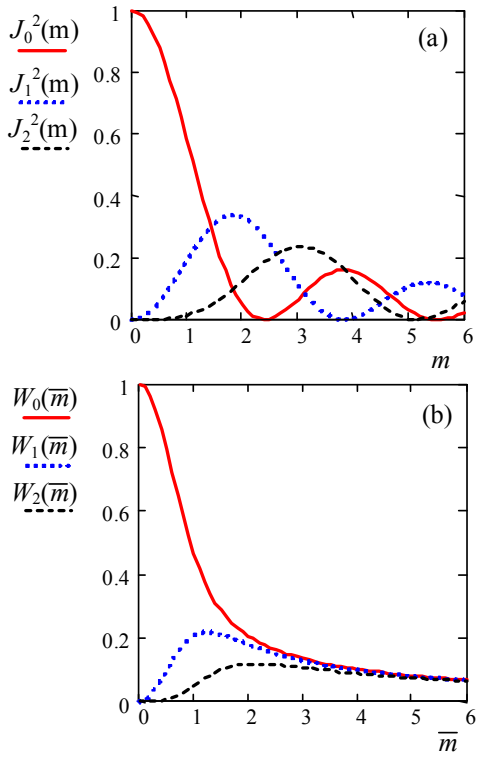

FIG. 1: (color on line) (a) The dependence of the intensities of the central component (solid line in red), first satellite (dotted line in blue), and second satellite (dashed line in black) on the modulation index m for the coherent model. (b) The dependence of the averaged intensities of the central component (solid line in red), first satellite (dotted line in blue), and second satellite (dashed line in black) on $\bar{m}$, which is the square root of the modulation index deviation $\langle m^2 \rangle$, for the incoherent model.

distances that are multiples of the oscillation frequency. The intensity of the nth sideband is given by the square of the Bessel function $J_n^2(m)$. According to this theoretical prediction the line intensities oscillate with increase of the modulation index m, see Fig. 1(a). For example, the first sidebands, whose intensities are proportional to $J_{\pm 1}^2(m)$ take their global maxima when $m = 1.8$, while the intensity of the central component $J_0^2(m)$ is zero if $m = 2.4$. A model of uniform and phased vibrations of all the nuclei in the absorber is named the coherent model. Unfortunately, experiments with powder absorbers did not demonstrate oscillatory dependence of the sideband intensities on the modulation index. Even in many experiments the intensity of the central component was always the strongest, while the intensity of the satellites, initially increasing with the modulation amplitude increase, then

monotonically decreased as a function of m. Meanwhile, experiments with stainless steel foil [31, 32] showed appreciable decrease of the central component of the spectrum to the level of the sidebands with increase of the modulation index m and revealed some oscillating dependencies of the spectral components on m.

B. Incoherent model

The incoherent model was proposed [26–30] to explain the discrepancy between the coherent model and the experiment. It is based on the Abragam model [35] suggesting that the motion of individual nucleus in the absorber along the propagation direction $\mathbf{z}$ of γ photon can be described as $a_z(t) = a_c \cos(\Omega t + \psi) + a_s \sin(\Omega t + \psi)$, where a_c and a_s are the amplitudes of in phase and out of phase oscillations [27]. For the ensemble of nuclei, distributed homogeneously in the absorber, the amplitudes a_c and a_s are Gaussian-distributed, centered at zero, and independent, i.e.,

$$G(a_{c,s}, \langle a_{c,s}^2 \rangle) = \frac{\exp\left(-\frac{a_{c,s}^2}{2\langle a_{c,s}^2 \rangle}\right)}{\sqrt{2\pi \langle a_{c,s}^2 \rangle}}, \tag{12}$$

where $\langle a_{c,s}^2 \rangle$ is variance, which is not zero, while mean values of the amplitudes are zero, $\langle a_{c,s} \rangle = 0$. The vibration amplitude and phase are $a = \sqrt{a_c^2 + a_s^2}$ and $\psi_r = \psi + \tan^{-1}(a_s/a_c)$, respectively. If $\langle a_c^2 \rangle = \langle a_s^2 \rangle = \overline{a^2}$, the vibration amplitude is distributed as

$$P_R(a, \overline{a^2}) = \int_{-\infty}^{+\infty} da_c \int_{-\infty}^{+\infty} da_s \frac{\exp\left(-\frac{a_c^2 + a_s^2}{2\overline{a^2}}\right)}{2\pi \overline{a^2}} \delta(a - \sqrt{a_c^2 + a_s^2}). \tag{13}$$

Since the amplitudes a_c and a_s are not correlated, the phase ψ_r is randomly distributed over the interval 0 and 2π. Therefore, in a polar coordinate system (r, ψ_r), where $r = \sqrt{a_c^2 + a_s^2}$, this distribution is transformed to

$$P_R(a, \overline{a^2}) = \int_0^{2\pi} d\psi_r \int_{-\infty}^{+\infty} r dr \frac{\exp\left(-\frac{r^2}{2\overline{a^2}}\right)}{2\pi \overline{a^2}} \delta(r - a), \tag{14}$$

which gives the Rayleigh distribution

$$P_R(a, \overline{a^2}) = \frac{a}{\overline{a^2}} \exp\left(-\frac{a^2}{2\overline{a^2}}\right). \tag{15}$$

Averaging the intensity of the nth sideband with this distribution,

$$W_n(\overline{m}) = \int_0^{\infty} P_R(a, \overline{a^2}) J_n^2\left(\frac{2\pi a}{\lambda}\right) da, \tag{16}$$

one obtains

$$W_n(\overline{m}) = e^{-\langle m^2 \rangle} I_n \left(\langle m^2 \rangle \right), \tag{17}$$

where $\langle m^2 \rangle = (2\pi/\lambda)^2 \overline{a^2}$ and $\overline{m} = \sqrt{\langle m^2 \rangle}$. The dependence of the components $W_n(\overline{m})$ on $\overline{m}$ is shown in Fig. 1(b) for $n = 0$, 1, and 2 .

III. THE ARGUMENTS FOR A REVISION OF THE INCOHERENT MODEL

Actually the spectra of powder absorbers [27] and thin films, for example, stainless steel foil, experiencing mechanical vibrations, [28, 30–32, 37] are quite different. Usually these absorbers are glued on the surface of the transducer, fed by the oscillating voltage. The transducers, made from piezo-crystal (for example, quartz) [23, 24, 26–34] or piezo-polymer-film (for example, a polyvinylidene fluoride - PVDF), also produce different spectra since the conversion factor of the PVDF drive is more than ten times larger than that of quartz [38]. Meanwhile, the Rayleigh distribution has only one parameter, which is a variance of the displacement amplitude $\overline{a^2}$, specifying also the values $\langle m^2 \rangle$ and $\overline{m}$. However, in general the distribution of amplitudes and phases of the nuclear vibrations should depend on the construction of the absorber-transducer. Therefore, it is hard to expect that by one model with a single parameter it would be possible to fit qualitatively different experimental spectra.

In addition to the arguments given above, the incoherent model contradicts the observation of time domain spectra, which are obtained for γ rays from the vibrated source by filtering trough a single line absorber [23, 24]. Similar experiments were performed with the vibrated absorber and the source moved only by Mössbauer drive [10, 18, 19, 25]. In Ref. [24], Monahan and Perlow developed a theory of quantum beats of recoil-free γ radiation, which is emitted by frequency-modulated source and transmitted through a resonant absorber. It follows from their model that if random phase ψ_r and amplitude a of the mechanical vibrations are statistically independent and ψ_r is randomly distributed over the interval 0 and 2π, no quantum beats will be observed. If ψ_r is distributed normally about $\psi_r = 0$ with variance $\langle \psi_r^2 \rangle$, then amplitudes of the harmonics in time domain spectra significantly decrease with increase of the number of the harmonic. Since quantum beats of frequency modulated γ-rays, which are transmitted through the resonant absorber, are reliably observed [23, 24], the phase ψ_r is not randomly distributed over the interval 0 and 2π.

Moreover, no extra damping of the second harmonic with respect to the first harmonic in the harmonic composition of the time-dependent counting rate of the filtered γ-photons was reported in Ref. [23, 24]. Thus, we conclude that no random jitter of the phase ψ_r around $\psi_r = 0$ with a small variance $\langle \psi_r^2 \rangle$ is present.

We can add to the arguments of Perlow and Monahan that if the phase is random, then not only the amplitudes of quantum beats of the vibrational sidebands, observed in time domain spectra [23, 24], are reduced or even could vanish due to the phase fluctuation of the vibrations, but also frequency domain spectra must be broadened. This can be shown if we consider the radiation field $E_S(t - t_0)$ with vibrational sidebands, described by Eq. (2). It is natural to suppose that the phase ψ_r and modulation index $m = 2\pi a/\lambda$, which is proportional to the vibration amplitude a, are statistically independent. Therefore, the averaging over these parameters can be made independently and the contribution of the amplitude and phase fluctuations are factorized. Below we consider the contribution of the phase fluctuations.

It is well known in quantum optics that if the phase ψ_r of the coherent field

$$E_n(t) = E_c e^{-i\omega_S t + in(\Omega t + \psi_r)} \tag{18}$$

randomly fluctuates in time, then the spectrum of the field is broadened, see, for example, Ref. [39] and plenty references therein.

Suppose that phase fluctuation follows phase diffusion process when phase changes by small jumps and due to a random walk the phase ψ_r can go very far from its initial value taking all values between 0 and 2π with equal probability. In this model it is assumed that the next value of phase has a Gaussian distribution, which is symmetric around the prior value with variance $\langle \delta\psi_r^2 \rangle$. Phase diffusion process produces spectral broadening of the field $E_n(t)$. If, for example, without phase fluctuation the field spectrum was delta-like, then due to the random walk of phase the power spectrum of the field becomes Lorentzian with the width $\nu_n = n^2 \langle \delta\psi_r^2 \rangle / \tau_0$, where $\langle \delta\psi_r^2 \rangle$ is a mean square value of the size of the phase jump and τ_0 is a mean dwell time between successive phase jumps [39].

The phase diffusion model predicts that the central component of the field (2) with $n = 0$ is not spectrally broadened, while sidebands are broadened. The broadening of the sidebands increases proportionally to n^2. To take this broadening into account we have to replace the halfwidth of the spectral components of the field $\Gamma_0/2$ in Eqs. (3) and (4) by

$\gamma_n = \Gamma_0/2 + n^2 \langle \delta\psi_r^2 \rangle / 2\tau_0$, where n is the number of the sideband. Usually, all experimental spectra of the vibrated absorbers are fitted by the set of Lorentzians with the same width. However, nobody reported progressive broadening of the satellites. In Sec. V, Subsec. A we also report that no difference between the widths of the sidebands and the central component is found.

There is another model assuming that the phase after a jump takes any value between 0 and 2π with equal probability. This uncorrelated process predicts [39] the same extra broadening for all sidebands except the central component with $n = 0$. According to this model, the Lorentzian extra broadening of the sidebands is equal to $1/\tau_0$ [39]. Also, the marked difference between the width of the central line and sidebands has not been yet reported.

Thus, we conclude that fast time variation of phase of the mechanical vibration is not present in the vibrated absorber or source if sidebands with the same width as the central line are observed.

IV. THE MODEL OF COHERENT VIBRATIONS WITH NONZERO AVERAGE AMPLITUDE

The Rayleigh distribution is derived with the assumption that the amplitudes a_c and a_s are Gaussian-distributed, centered at zero, and independent, see Sec. II. This means that $a_{c,s} = 0$ has maximum probability. However, if we move a thin absorber by a coherently vibrated transducer, it is better to suppose that the distribution of the vibration amplitudes is centered at some value $a_0 \neq 0$. Below, following the arguments given in Sec. III, we assume that displacements along $\mathbf{z}$ direction are described by $a_z = a \cos \Omega t$, where for simplicity we set $\psi = 0$. Then, it is natural to suppose that the amplitude a is Gaussian-distributed and centered at a_0 with variance $\langle \delta a^2 \rangle$, i.e.,

$$G(a, a_0) = \frac{\exp\left(-\frac{(a-a_0)^2}{2\langle \delta a^2 \rangle}\right)}{\sqrt{2\pi \langle \delta a^2 \rangle}}. \tag{19}$$

Usually, Gaussian distribution is defined for a varied in the domain $(-\infty, \infty)$. However, a is the amplitude, which is defined for positive values. Therefore, we restrict domain of the amplitude variation by positive values $(0, \infty)$. To keep the same overall density of our

distribution we normalize it to

$$N\left(a_0\right)=\int_0^{+\infty} G\left(a,a_0\right)da \tag{20}$$

and obtain

$$G_{\mathrm{norm}}\left(a,a_0\right)=\frac{\exp\left(-\frac{(a-a_0)^2}{2\langle\delta a^2\rangle}\right)}{N\left(a_0\right)\sqrt{2\pi\left\langle\delta a^2\right\rangle}}. \tag{21}$$

This distribution needs further modification since the intensity of the nth sideband

$$W_n(a_0)=\int_0^{\infty} G_{\mathrm{norm}}\left(a,a_0\right)J_n^2\left(\frac{2\pi a}{\lambda}\right)da, \tag{22}$$

is not zero for $n\neq 0$ if $a_0=0$ and $\langle\delta a^2\rangle\neq 0$. This discrepancy appears due to the fact that the probability $G_{\mathrm{norm}}\left(a,a_0\right)$ does not become zero if a_0 is zero, i.e., when no oscillations should be present. The origin of this discrepancy comes from the variance $\langle\delta a^2\rangle$, which should be zero if $a_0=0$. To fix this problem we define variance as $\langle\delta a^2\rangle=(\sigma a_0)^2$, which means that variance is specified in a percentage σ of the mean value of the amplitude a_0. Then, if $a_0=0$, the variance is also zero. With these modifications we obtain the following expression for the intensity of the nth sideband

$$\overline{W}_n\left(m_0,\sigma\right)=\frac{\sqrt{\frac{2}{\pi}}\int_0^{\infty}\exp\left[-\frac{1}{2}\left(x-\frac{1}{\sigma}\right)^2\right]J_n^2(\sigma m_0 x)dx}{1+\mathrm{erf}\left(\frac{1}{\sqrt{2}\sigma}\right)}, \tag{23}$$

where $m_0=2\pi a_0/\lambda$.

If $\sigma=0.1$ the variance $\langle\delta a^2\rangle$ is much smaller than a_0^2. Then, the distribution $G_{\mathrm{norm}}\left(a,a_0\right)$ is close to a delta-like [see Fig. 2(a)], and the dependence of the intensity $\overline{W}_n\left(m_0,\sigma\right)$ on m_0 [see Fig. 3(a)] is very similar to that shown in Fig. 1(a) for the coherent model. If $\sigma=0.72$, the variance $\langle\delta a^2\rangle$ is comparable with a_0^2. Then, the distribution $G_{\mathrm{norm}}\left(a,a_0\right)$ is close to the Rayleigh distribution [see Fig. 2(b)], and the intensity $\overline{W}_n\left(m_0,\sigma\right)$ depends on m_0 [see Fig. 3(a)] similar to that shown in Fig. 1(b) for the incoherent model.

V. EXPERIMENT

Our experimental setup is based on an ordinary Mössbauer spectrometer. The source, ^{57}Co:Rh, is mounted on the holder of the Mössbauer drive, which is used to Doppler-shift the frequency of the radiation field emitted by the source nucleus.

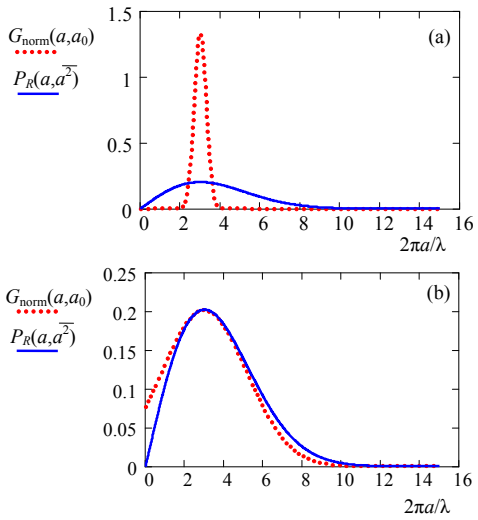

FIG. 2: (color on line) The dependence of our distributions $G_{\rm norm}\,(a, a_0)$ (dotted line in red) and Raylegh distribution (solid line in blue) on the amplitude of the displacement a. In both plots $a_0 = \sqrt{\overline{a^2}} = 3\lambda/2\pi$, which corresponds to $m_0 = 3$. Parameter σ is 0.1 in (a), and 0.72 in (b).

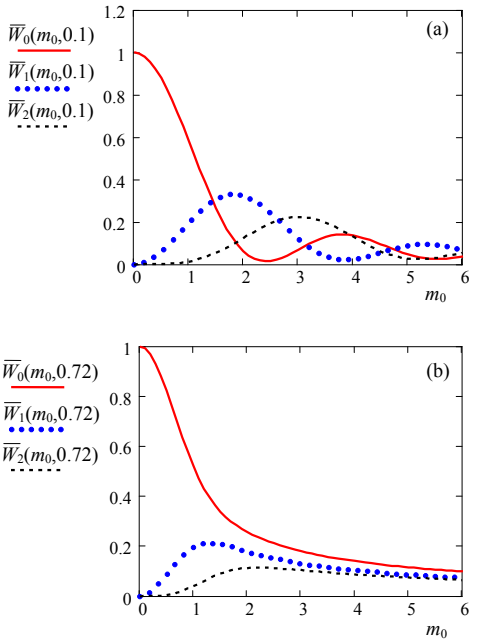

FIG. 3: (color on line) Dependence of the intensity $\overline{W}_n\,(m_0, \sigma)$ of the n-th sideband on m_0 for our model. Parameter σ is 0.1 in (a) and 0.72 in (b). Solid line (in red) corresponds to $n = 0$, dotted line (in blue) shows the dependence for $n = 1$, and dashed line (in black) corresponds to $n = 3$.

We carried out experiments with two different absorbers. The first absorber was made of enriched (95% of ^{57}Fe) $K_4Fe(CN)_6 \cdot 3H_2O$ powder with effective thickness 13.2. The enriched powder was produced by M. N. Mikheev Institute of Metal Physics, Ural Branch of Russian Academy of Sciences, Yekaterinburg. The powder was mechanically pressed to the surface of the transducer. Therefore, in the experiments with powder the source was placed below the absorber and the detector was mounted above the absorber. This vertical geometry of the experiment allowed to consider a powder as a grained substance just freely jumping up and down under the influence of the vibrating transducer.

As a transducer we used in both experiments a polyvinylidene fluoride (PVDF) piezo polymer film (thickness 28 μm, model LDT0-28K, Measurement Specialties, Inc.). Several piezoelectric transducer constructions were tested to achieve the best performance. The best of them was a piece of 28 μm thick, 10×12 mm polar PVDF film coupled to a plexiglass backing of ∼2 mm thickness with epoxy glue. The PVDF film transforms the sinusoidal signal from the radio-frequency (RF) generator into a uniform vibration of the absorber nuclei.

The second absorber was stainless steel foil from Alfa Aesar (production No. 41580), 25-μm-thick, Type 304 with a natural abundance (2.119%) of ^{57}Fe [40, 41]. The composition of the stainless-steel foil is Fe:Cr:Ni; 70:19:11 wt%. Optical depth of the second absorber is $T_A = 5.18$. The stainless-steel foil is glued on the PVDF piezotransducer. Therefore, the experiments with stainless-steel foil were carried out in a standard horizontal geometry.

A. Powder absorber

Powder absorber has a single absorption line, shown in Fig. 4. Experimental spectrum is well fitted by expression [42]

$$N_{\rm out}(\Delta) \propto e^{-\mu}[(1 - f_S) + f_S B_0(\Delta)], \tag{24}$$

where f_S is the recoil-free fraction of the source, $\exp(-\mu)$ is the absorption factor due to electrons, and $B_0(\Delta)$ is defined in Eq. (11). The effective thickness of the absorber is $T_A = 13.2$, isomer shift is -0.1 mm/sec. The effective thickness was found using the fitting of the transmission integral to the experimental spectrum [43].

Initially we supposed that powder absorber would behave as a sand placed on the vibrated

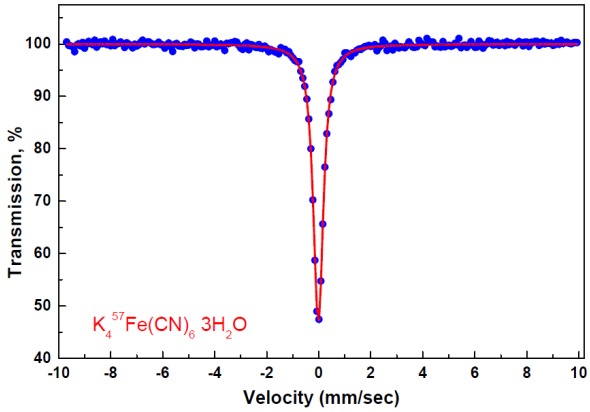

FIG. 4: (color on line) Absorption spectrum of the single-line powder absorber $K_4Fe(CN)_6 \cdot 3H_2O$. Blue dots are experimental data and solid line (in red) is the theoretical fitting to Eq. (24).

transducer. Then, powder grains should randomly jump and fall down to the vibrated surface with phase depending on the size and weight of the grains. Therefore, we expected that single parent line should not split in sidebands, which must be strongly broadened due to the random motion of grains, and hence vibrational sidebands could give only a broadening of the wings of the absorption line. However, in a wide range of the vibration frequencies from 5 MHz to 45 MHz we observed the sidebands. We used the same voltage, 10V, supplied from RF generator, except for high frequencies (35 , 40, and 45 MHz). For them we elevated voltage up to 16V since the amplitudes of the sidebands significantly reduced with increase of the RF frequency and we could observe for high frequencies only first two sidebands $\omega_S \pm \Omega$ with very small intensities.

Initially, we fitted the spectra by a parent line accompanied by n sidebands spaced by frequency Ω. We modeled n and $-n$ sidebands as a doublet with the same width and intensity. The fitting parameters were the depth of the central line and each doublet, and the width of the central line and the doublets. We allowed in fitting procedure that the widths and intensities of all spectral components (central line and the doublets) may be different. All the spectral components are approximated by Lorentzians. As a result of experimental spectra fitting, we did not find the difference in the widths of the central line and the sidebands.

Then, we made fitting of the experimental data to the Abragam model and our model. The results are shown in Fig. 5, where in (a)-(c) the Abragam model is used, while in (d)-

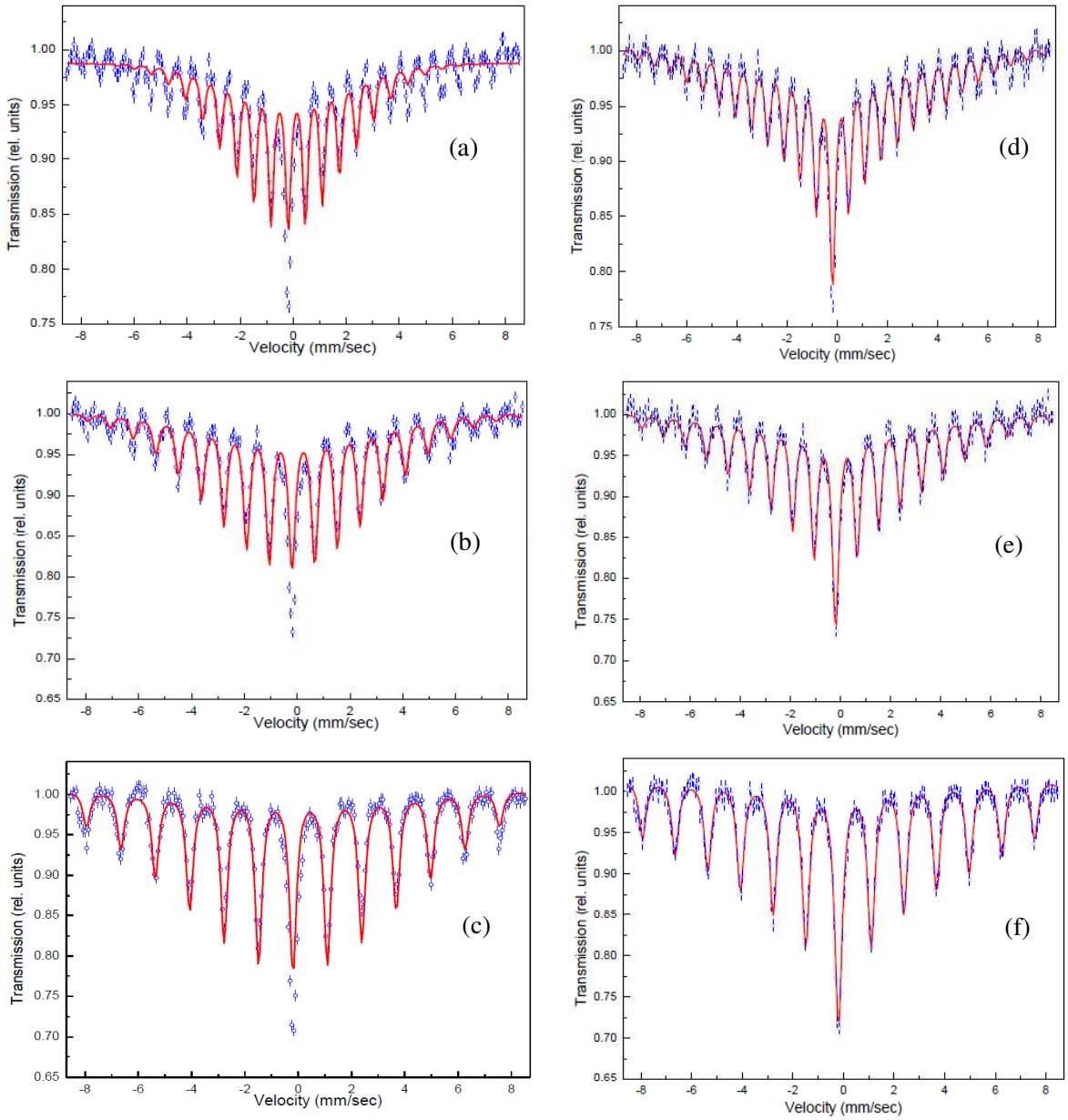

FIG. 5: (color on line) Absorption spectra of the powder absorber vibrated with the frequency Ω equal to 7.5 MHz (a) and (d), 10 MHz (b) and (e), and 15 MHz (c) and (f). Dots are experimental data, solid line (in red) is the theoretical fitting to the Abragam model (a)-(c) and our model (d)-(f). For the Abragam model the modulation index $m_0 = 2\pi\sqrt{\overline{a^2}}/\lambda$ is 3.42 in (a), 3.66 in (b), and 3.39 in (c). For our model we obtained m_0, which is 5.6 in (d), 4.3 in (e), and 4.7 in (f).

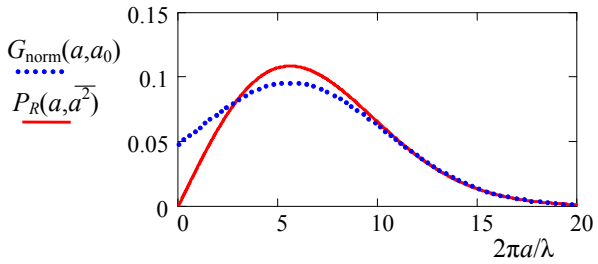

FIG. 6: (color on line) The functional dependence of our distribution $G_{\text{norm}}(a, a_0)$ on the amplitude of the displacement a for $m_0 = 5.6$ and $\sigma = 0.85$ (dotted line in blue). The Rayleigh distribution for the value of $\sqrt{\overline{a^2}} = a_0$, where $a_0 = m_0\lambda/2\pi$, is shown for comparison by the solid line (in red).

(f) our model is applied to fit data. Abragam model gives bad fitting except frequencies Ω equal or higher than 35 MHz when we observed only three lines, i.e., the central component and two sidebands. For frequencies below 35 MHz, especially the central component and components near to it, are in a strong disagreement with the Abragam model. The spectra calculated according to our model agree well with experiment.

According to our model, for the same voltage from RF generator (10V), mean value of the modulation index m_0 takes maximum value $m_0 = 5.6$ for $\Omega = 7.5$ MHz and then decreases with increase of the frequency Ω. For example, for $\Omega = 15$ MHz we have $m_0 = 4.7$, while for $\Omega = 20$ MHz mean value of the modulation index drops almost two times, i.e., $m_0 = 2.6$. The smallest value of the modulation index $m_0 = 0.25$ was obtained for $\Omega = 40$ MHz, when the voltage was even elevated to 16V. Such a dependence of m_0 on the modulation frequency Ω could be explained by maximum efficiency of the process inducing mechanical vibrations of the powder near $\Omega = 7.5$ MHz.

The best fitting of our theoretical predictions to the experimental data is obtained with $\sigma = 0.85$, which corresponds to the value of the square root of variance $\sqrt{\delta a^2}$ equal to 85% of the mean amplitude a_0. This reflects a large spread of the amplitudes of the mechanical vibrations a around a_0. Comparison of our distribution $G_{\text{norm}}(a, a_0)$ with the Rayleigh distribution $P_R\left(a, \overline{a^2}\right)$ for $m_0 = 5.6$ and $\sigma = 0.85$ is shown in Fig. 6. Our distribution looks close to the continuous uniform distribution for the values of a between 0 and 2λ.

The observed spectra of the powder absorber could be explained as follows. Since our powder is hygroscopic, it does not behave as a dry sand. Actually in the experiment the powder is compressed in a tablet-like substance, which shows small adhesion to the sur-

face of the PVDF transducer. This explains the coherent motion of the powder grains. Their difference in size and orientation of the crystalline axis with respect to the direction of the displacement z could be a reason of almost continuous uniform distribution of the displacement amplitudes.

B. Stainless-steel absorber

Stainless-steel (SS) foil has also a single absorption line (see Fig. 7). It is well fitted by the theoretical prediction Eq. (24) with optical thickness $T_A = 5.18$ and isomer shift -0.04 mm/sec.

The spectra obtained for the vibrated stainless steel absorber are quite different from those observed for the powder absorber. They demonstrated some features typical for the coherent model, see Fig. 8. However, these spectra could not be reasonably well described by the simple coherent model.

In Ref. [32], it was assumed that some part of nuclei in the absorber vibrate coherently with the same amplitude, while another part of nuclei also participate in the coherent vibration, but for them the mean square displacement value changes from nucleus to nucleus. We tried to fit experimental data for SS absorber to the model [32], where experimental spectra are compared with theoretical predictions assuming a mixture (a simple sum with different weights) of the coherent and incoherent models. However, this method did not allow to obtain good fitting. Therefore, we decided to fit experimental spectra to our model. The results of fitting are shown in Fig. 8.

C. Model for SS foil vibration

The fitting allowed us to find the parameter σ. Figure 9 shows comparison of our distribution for this parameter with the Rayleigh distribution for the modulation index $m_0 = 3.01$. It is clear that for SS absorber the distribution of the displacement amplitude looks bell shape. Such a distribution gives a hint about a real distribution of the vibration amplitudes along the surface of the absorber. Before constructing this real distribution we give some arguments in support of the model.

PVDF film is glued on the solid plexiglass backing. Oscillating voltage forces the film to

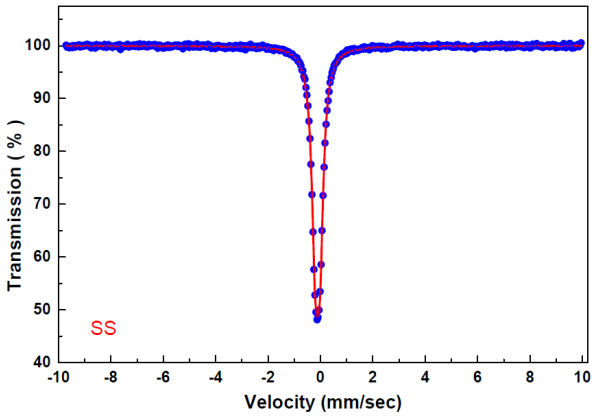

FIG. 7: (color on line) Absorption spectrum of the stainless steel absorber. Blue dots are experimental data and solid line (in red) is the theoretical fitting to Eq. (24).

change its thickness making it thicker or thinner. We may assume that the lateral size of the film also oscillates. However, the solid backing resists the lateral changes of the film. Therefore, we may assume that amplitude of the displacement is larger in the center of the film and smaller at the edges.

To avoid complications we model SS film as having a form of a disk with radius r_0. This disk vibrates such that displacement has a maximum at the center and decreases to the edges. All elements of the disk vibrate with the same frequency and phase. We assume that the amplitudes of the vibrations are distributed according to a bell-shape function, slightly resembling $G_{\rm norm}(a, a_0)$, as

$$a(r) = a_0 \cos\left(\xi \frac{\pi}{2} \frac{r}{r_0}\right), \tag{25}$$

where a_0 is a maximum amplitude at the disk center, r is a distance from the center, and ξ is a parameter, which specifies the difference between the amplitudes at the center, $a(0) = a_0$, and edges, $a(r_0) = a_0 \cos(\xi\pi/2)$. If $\xi \ll 1$, then this difference is small and the distribution is close to the uniform distribution along the absorber. If $\xi = 1$, then the amplitude at the edges of the disk is zero. In both cases the distribution is a bell shape as it is designed.

We assume that a beam of γ-radiation is transversely uniform and covers the whole disk. In some cases the beam diameter $2r_{\rm beam}$, which is defined by the collimator aperture and the distance from the source to absorber, could be smaller than the disc diameter $2r_0$. In both cases, for wide ($r_{\rm beam} \approx r_0$) or narrow ($r_{\rm beam} \ll r_0$) γ-beam, the intensity of the transmitted radiation for the nth sideband is described by the integral over the beam area $S_0 = \pi r_{\rm beam}^2$,

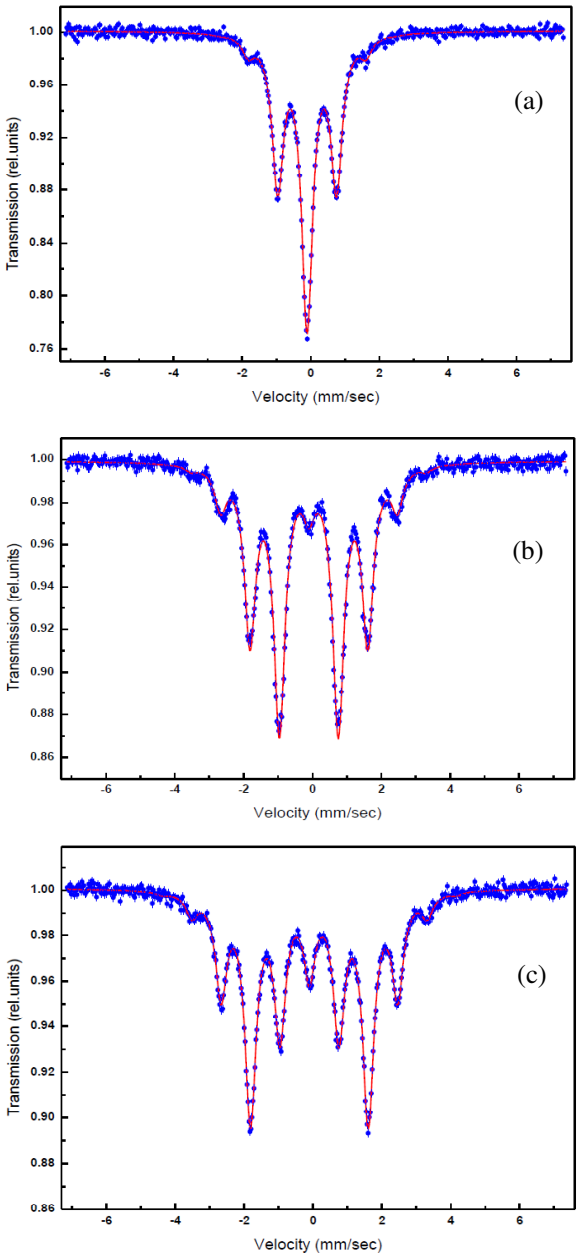

FIG. 8: (color on line) Absorption spectra for SS absorber vibrated with frequency 10 MHz. The applied voltage is 6.2V in (a), 12.2V in (b), and 15.4V in (c). Dots are experimental data, solid line (in red) is the theoretical fitting by our model. Fitting parameters are $m_0 = 1.19$ and $\sigma = 0.18$ in (a), $m_0 = 2.38$ and $\sigma = 0.16$ in (b), and $m_0 = 3.01$ and $\sigma = 0.16$ in (c).

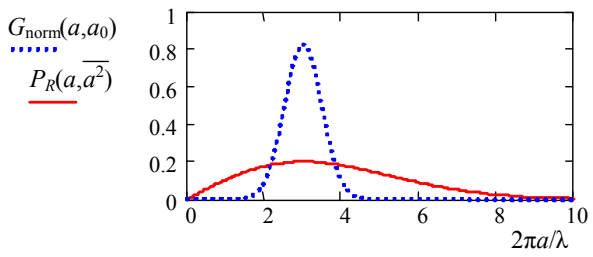

FIG. 9: (color on line) Comparison of our distribution $G_{\rm norm}\,(a, a_0)$ (dotted line in blue) with the Rayleigh distribution (solid line in red) for the modulation index $m_0 = 3.01$ and $\sigma = 0.16$.

i.e.,

$$\widetilde{W}_n(m_0, r_{\rm beam}, \xi) = \frac{1}{S_0}\int_0^{2\pi} d\varphi \int_0^{r_{\rm beam}} r dr J_n^2\left[m_0 \cos\left(\xi\frac{\pi}{2}\frac{r}{r_0}\right)\right], \tag{26}$$

where $m_0 = 2\pi a_0/\lambda$ and angle φ defines a direction on the disk surface of the vector $\mathbf{r}$ with a length r and origin in the disk center. This integral is reduced to

$$\widetilde{W}_n(m_0, r_{\rm beam}, \xi) = \frac{2}{r_{\rm beam}^2}\int_0^{r_{\rm beam}} J_n^2\left[m_0 \cos\left(\xi\frac{\pi}{2}\frac{r}{r_0}\right)\right] r dr, \tag{27}$$

If $r_0 = r_{\rm beam}$, the parameter r_0 can be excluded from the model by introducing a variable $x = r/r_0$. Then, Eq. (27) is simplified as

$$\widetilde{W}_n(m_0, \xi) = 2\int_0^1 J_n^2\left[m_0 \cos\left(\xi\frac{\pi}{2}x\right)\right] x dx. \tag{28}$$

Thus, the parameter ξ defines a measure of homogeneity of the vibration amplitudes across the beam of γ-radiation. If $\xi \to 0$, the vibration amplitudes are almost the same for all nuclei exposed to γ-radiation. If $\xi \to 1$, the amplitudes are very different. Our modeling assumption about the shape of the absorber is not important if $2r_{\rm beam}$ is smaller than the lateral dimensions of the absorber.

The dependence of the intensities of the spectral components $\widetilde{W}_n(m_0, \xi)$ for $n = 0$, 1, and 2 is shown in Fig. 10. For small ξ (i.e., $\xi = 0.1$) this dependence is close to that inherent to the coherent model since the vibration amplitudes of nuclei are almost the same. For the value $\xi = 0.95$ the dependence resembles the predictions of the Abragam model.

The similarity of the results of the disk and Abragam models for $\xi \to 1$ originates from the similarity of the structure of the integrals in Eqs. (16) and (28), where the Bessel function is averaged with the function proportional to $a\ da$ in Eq. (16) and to $x\ dx$ in Eq. (28). Another common feature is that both distributions are centered at the value of the

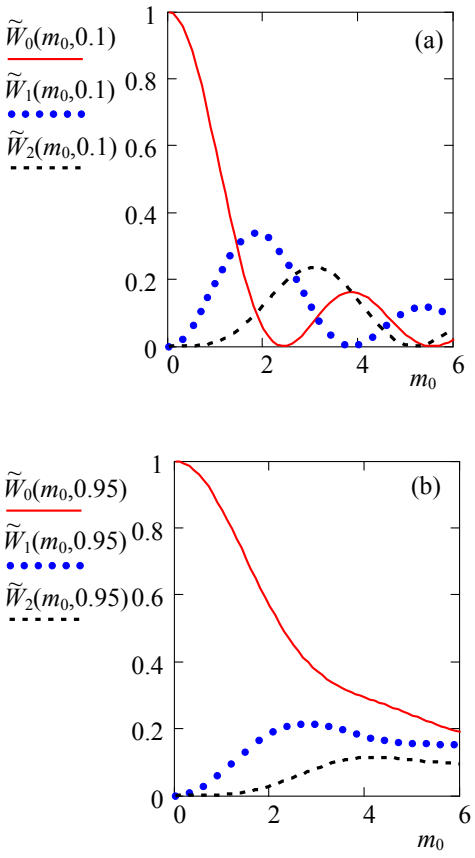

FIG. 10: (color on line) Dependence of the intensity $\widetilde{W}_n(m_0,\xi)$ on m_0 for the model of disk vibration. Parameter ξ is 0.1 in (a) and 0.95 in (b). Solid line (in red) corresponds to $n = 0$, dotted line (in blue) shows the dependence for $n = 1$, and dashed line (in black) corresponds to $n = 3$.

integration variable, which is zero, i.e., $a = 0$ in Eq. (16) and $x = 0$ ($r = 0$) in Eq. (28). However, these distributions are very different in one important point. Rayleigh distribution is based on the assumption that the probability has maximum for zero displacement a. Our distribution assumes that the displacement amplitude has maximum value $a_0 \neq 0$ when radius r, which is the averaging parameter, is zero.

Experimental spectra are described much better by the theoretical prediction, based on the disk model, compared with our first model. Therefore, we conclude that the disk model is more appropriate for description of the SS foil vibration. The fitting parameter ξ is quite small. This means that dispersion of the displacements along the surface of the film is also small.

D. Absorber with a lead mask

We may assume that if the disk model is more adequate than other models, then it could help to look for experimental conditions when the vibration amplitudes of nuclei, exposed to gamma radiation, could be made even more homogeneous. If we would increase the homogeneity, then the experimental spectra would be even more closer to those, which follow from the coherent model.

According to the disk model the simplest way to increase the homogeneity of the displacement is to remove the contribution of nuclei located far from the absorber center. This could be done by placing a lead mask with a small round hole in the front of absorber and locate the mask such that the aperture coincides with the absorber center.

To make sure that our assumptions are correct, we measured several spectra with different diameter of aperture in the mask. According to our expectations the spectra must change with the change of the size of the aperture.

The absorption spectra of the absorber with the lead mask are shown in Fig. 11. Diameter of the hole in the mask was varied from 2.45 mm to 1.1 mm. These spectra are obtained for the same frequency and voltage of the the RF generator. In the coherent model the central component becomes zero for the modulation index $m = 2.4$. We suppose that spectra in Fig. 11 are obtained with the modulation index quite close to this value. Therefore, the observed lessening of the central component of the absorption spectra with diminution of the hole diameter in the lead mask proves that scattering of the vibration amplitudes of nuclei, exposed to γ-radiation, becomes smaller with decreasing size of the hole. At the same time the relative intensities of the sidebands increase with diminution of the hole diameter.

For the smallest hole in the lead mask, the disk model gives the maximum value of the vibration amplitude $a_0 = 36.7$ pm at the disk center. The scattering parameter $\xi = 0.21$ for this hole is small. Therefore, the amplitude at the hole edge $a(r_0) = a_0 \cos(\xi\pi/2)$ is 34.7 pm, which differs from a_0 only by 2 pm. This 5% difference gives the accuracy of the displacement measurement with the smallest hole.

By this lead mask with the smallest hole (1.1 mm) we scanned the surface of the absorber. The obtained spectra are shown in Fig. 12. Since the spectra obtained with the lead mask having the smallest hole are very close to that predicted by the coherent model, we expect that such a scanning is capable to provide the information about distribution of the vibration

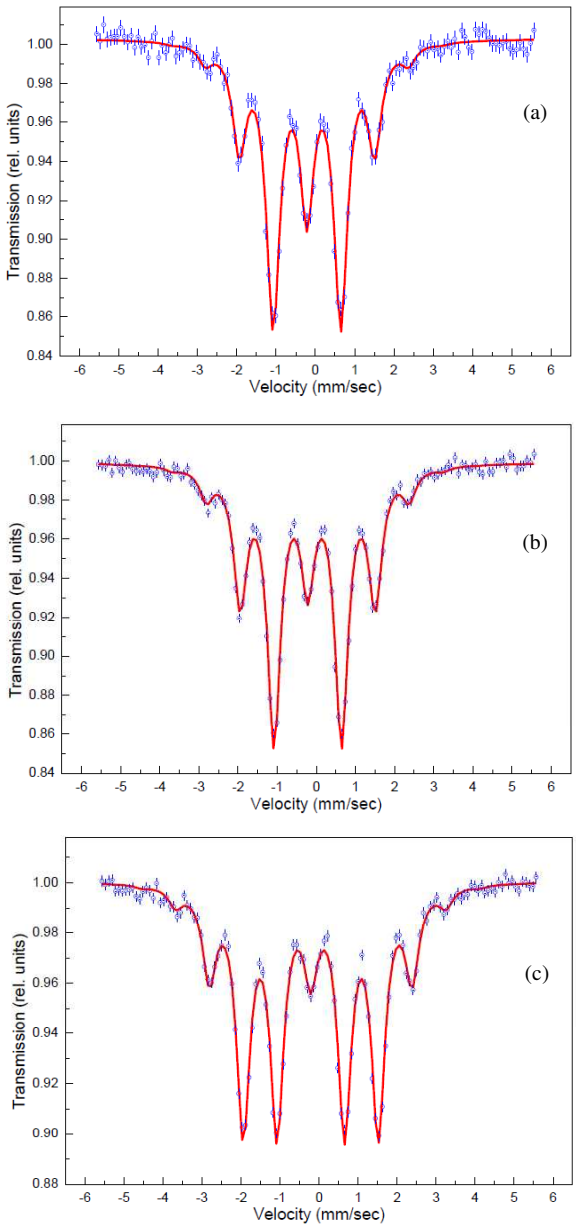

FIG. 11: (color on line) Absorption spectra for the SS absorber obtained with the lead mask. Diameter of the hole in the lead mask is 2.45 mm in (a), 1.7 mm in (b), and 1.1 mm in (c). The absorber is vibrated with frequency 10.7 MHz. Dots are experimental data, solid line (in red) is the theoretical fitting to the disk model. The values of the modulation index m_0 and parameter ξ are 1.85 and 0.27 in (a), 2.08 and 0.25 in (b), and 2.68 and 0.21 in (c), respectively. The difference between values of maximum amplitude $a_0 \sim m_0$ in (a) -(c) for the same voltage of RF generator can be explained by imperfect positioning of the mask aperture with respect to the center of the absorber in experiments with different masks.

amplitudes along the surface of the absorber. We obtained the following results. When the hole coincides with the center of the absorber we have the splitting of the parent line into sidebands, which corresponds to the modulation index $m = 2.67$, see Fig. 12(a). Positions of the hole slightly below the center and shifted to the left in (c) and right in (d) give reduction of the modulation index to the values $m = 2.37$ in (c) and $m = 2.35$ in (d). Since these values are close to each other we may conclude that transverse shift (left/right) of the hole does not show appreciable change of the vibration amplitude. If we move the hole further down from the center, the value of the modulation index reduces to $m = 1.74$, see Fig. 12(b).

VI. DISCUSSION

Our experimental results, obtained for SS foil, give a strong hint at the presence of longitudinal distribution of the displacement amplitudes along the surface of the absorber, while in the transverse direction the amplitudes are more homogeneous. Since PVDF film is drawn and polarized during its fabrication, it is natural to expect the difference of the displacements in longitudinal and transverse directions. Long polymer chains aligned along a particular direction give the origin to this asymmetry. Therefore, we assume that our disk model cannot describe perfectly all the details of the vibration of the PVDF film with SS foil. However this model is good to describe the experiments with the lead mask having a round hole. We plan to develop a strip model of the vibration, which could be more adequate. Future experiments with the lead mask, whose small hole is scanned over the surface of the absorber, could provide topographical information about amplitude distribution over the sample surface. We expect that this information could help to construct a adequate model of the sample displacements.

As regards the powder absorber, we could screen the powder through a set of grids to make the powder grains almost of the same size. We expect that experiments with such a homogeneous powder could elucidate the origin of the spectrum behavior of the vibrated powder.

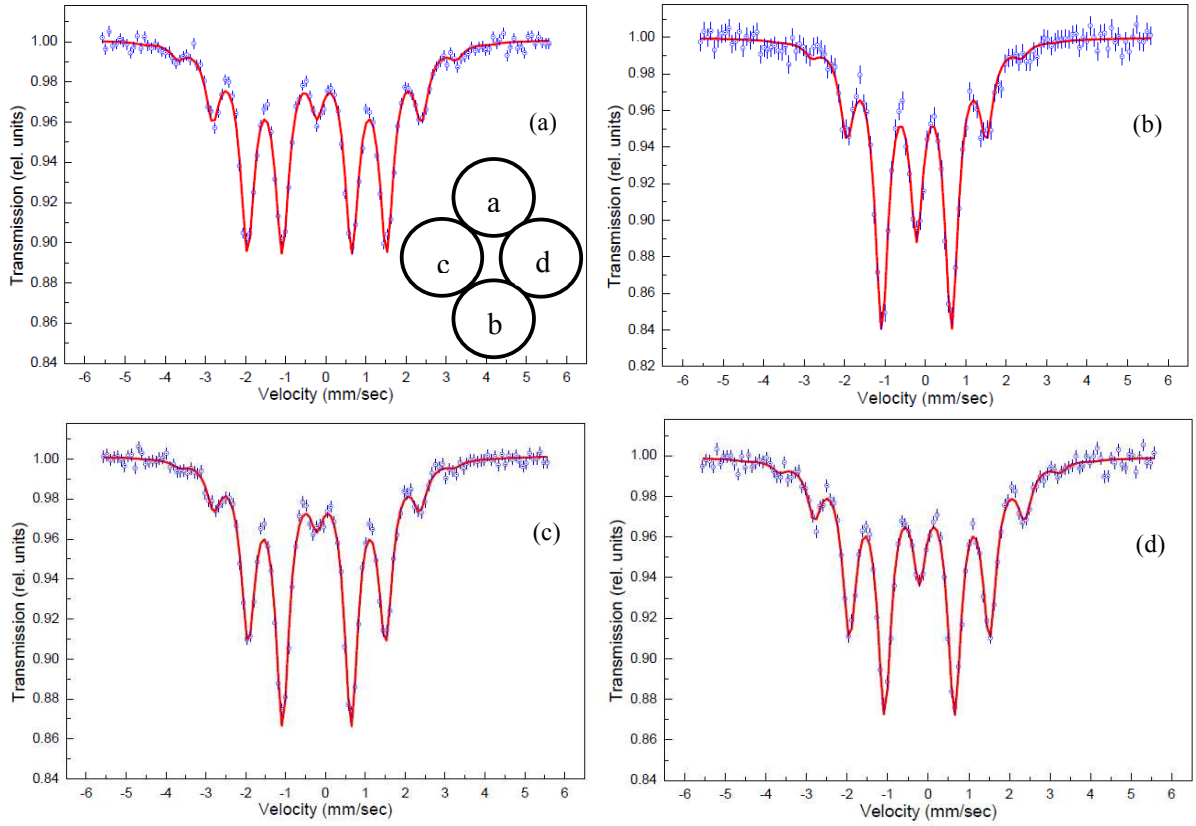

FIG. 12: (color on line) Absorption spectra for SS absorber obtained with the lead mask. The hole diameter in the mask is 1.1 mm. The hole position with respect to the absorber center is shown in the inset in (a) by black circles. Position of the upper circle coincides with the absorber center [spectrum (a)]. Other circles are moved away to the bottom [spectrum (b)], to the left and bottom [spectrum (c)], and to the right and bottom [spectrum (d)]. The absorber is vibrated with frequency of 10 MHz. The driving voltage is $V = 10.7$ V. Dots are experimental data, solid line (in red) is the theoretical fitting. The fitting parameters are $m_0 = 2.67$ and $\xi = 0.18$ in (a), $m_0 = 1.74$ and $\xi = 0.24$ in (b), $m_0 = 2.37$ and $\xi = 0.18$ in (c), and $m_0 = 2.35$ and $\xi = 0.27$ in (d).

VII. CONCLUSION

We studied the transformation of Mössbauer single parent line of the vibrated absorber into a reduced intensity central line accompanied by many sidebands. The intensities of the sidebands contain information about the amplitudes of the mechanical vibrations and their distribution along the surface of the absorber. Two absorbers, powder and SS foil, are experimentally studied. The experimental spectra are fitted to the model with two

parameters, i.e., the mean amplitude of the vibrations and their deviation, which is defined as a percentage of the mean amplitude. This model allows to conclude that the distribution of the displacements in powder absorber is close to the continuous uniform distribution with large scattering of the amplitudes, while for SS foil it is bell shaped with small scattering of the amplitudes. We proposed a distribution of the displacements in SS foil, which is related to the geometrical distribution of displacements along the surface of the foil. To verify our proposal we measured the spectra of the vibrated SS foil placing a lead mask with a small hole in it before the absorber. When the diameter of the hole in the mask is 1 mm, the displacements become almost uniform with 5% scattering around maximum value of the displacement. Therefore, the spectra can be described by the coherent model. This allows to measure the displacements along the surface of the vibrated foil with a few picometers accuracy. We expect that our finding will open a way for a new kind of spectroscopical measurements of extra small displacements.

VIII. ACKNOWLEDGEMENTS

This work was partially funded by the Russian Foundation for Basic Research (Grant No. 15-02-09039-a), the Program of Competitive Growth of Kazan Federal University, funded by the Russian Government, and the RAS Presidium Program "Fundamental optical spectroscopy and its applications."FGV acknowledges the support from the National Science Foundation (Grant No. PHY-1506467).

---

[1] T. E. Cranshaw, J. P. Schiffer, and A. B. Whitehead, Phys. Rev. Lett. **4**, 163 (1960).

[2] R. V. Pound, G. A. Rebka, Phys. Rev. Lett. **4**, 337 (1960).

[3] T. E. Cranshaw, J. P. Schiffer, Proc. Phys. Soc. **84**, 245 (1964).

[4] R. V. Pound, J. L. Snider, Phys. Rev. Lett. **13**, 539 (1964).

[5] R. V. Pound, J. L. Snider, Phys. Rev. **140**, B788 (1965).

[6] T. Katila, K.J. Riski, Phys. Lett. A **83**, 51 (1981).

[7] W. Potzel, C. Schäfer, M. Steiner, H. Karzel, W. Schiessl, M. Peter, G. M. Kalvius, T. Katila, E. Ikonen, P. Helistö, and J. Hietaniemi, Hyperfine Interactions **72**, 197 (1992).

[8] Y. Friedman, E. Yudkin, I. Nowik, I. Felner, H.-C. Wille, R. Röhlsberger, J. Haber, G. Wortmann, S. Arogeti, M. Friedman, Z. Brand, N. Levi, I. Shafir, O. Efrati, T. Frumson, A. Finkelstein, A. I. Chumakov, I. Kantor, and R. Rüffer, J. Synchrotron Rad. **22**, 723 (2015).

[9] Y. Friedman, I. Nowik, I. Felner, J. M. Steiner, E. Yudkin, S. Livshitz, H.-C. Wille, G. Wortmann, S. Arogeti, N. Levi, A. I. Chumakov, and R. Rüffer, EPL **114**, 50010 (2016).

[10] F. Vagizov, R. Shakhmuratov, and E. Sadykov, Phys. Status Solidi B **252**, 469 (2015).

[11] I. Kupenko, C. Strohm, C. McCammon, V. Cerantolla, K. Glazyrin, S. Petitgirard, D. Vasiukov, G. Aprilis, A. I. Chumakov, R. Rüffer, and L. Dubrovinsky, Review of Scientific Instruments, **86**, 114501 (2015).

[12] R. Röhlsberger, H-C. Wille, K. Schlage, and B. Sahoo, Nature **482**, 199 (2012).

[13] R. Röhlsberger, K. Schlage, B. Sahoo, S. Couet, and R. Rüffer, Science **328**, 1248 (2010).

[14] K. P. Heeg, H-C. Wille, K. Schlage, T. Guryeva, D. Schumacher, I. Uschmann, K. S. Schulze, B. Marx, T. Kämpfer, G. G. Paulus, R. Röhlsberger, and J. Evers, Phys. Rev. Lett. **111**, 073601 (2013).

[15] R. N. Shakhmuratov, F. G. Vagizov, and O. Kocharovskaya, Phys. Rev. A **87**, 013807 (2013).

[16] R. N. Shakhmuratov, F. G. Vagizov, J. Odeurs, and O. Kocharovskaya, Phys. Rev. A **80**, 063805 (2009).

[17] K. P. Heeg, J. Haber, D. Schumacher, L. Bocklage, H.-C. Wille, K. S. Schulze, R. Loetzsch, I. Uschmann, G. G. Paulus, R. Rüffer, R. Röhlsberger, and J. Evers, Phys. Rev. Lett. **114**, 203601 (2015).

[18] F. Vagizov, V. Antonov, Y. V. Radeonychev, R. N. Shakhmuratov, and O. Kocharovskaya, Nature **508**, 80 (2014).

[19] R. N. Shakhmuratov, F. G. Vagizov, V. A. Antonov, Y. V. Radeonychev, M. O. Scully, and O. Kocharovskaya, Phys. Rev. A **92**, 023836 (2015).

[20] P. Helistö, I. Tittonen, M. Lippmaa, and T. Katila, Phys. Rev. Lett. **66**, 2037 (1991).

[21] I. Tittonen, M. Lippmaa, P. Helistö, and T. Katila, Phys. Rev. B 47, 7840 (1993).

[22] R. N. Shakhmuratov, F. G. Vagizov, and O. Kocharovskaya, Phys. Rev. A **84**, 043820 (2011).

[23] G. J. Perlow, Phys. Rev. Lett. **40**, 896 (1978).

[24] J. E. Monahan, and G. J. Perlow, Phys. Rev. A **20**, 1499 (1979).

[25] R. N. Shakhmuratov, F. G. Vagizov, M. O. Scully, and O. Kocharovskaya, Phys. Rev. A **94**, 043849 (2016).

[26] S. L. Ruby, D. I. Bolef, Phys. Rev. Lett. **5**, 5 (1960).

[27] T. E. Cranshaw and P. Reivari, Proc. Phys. Soc. **90**, 1059 (1967).

[28] J. Mishroy and D. I. Bolef, Mössbauer Effect Methodology, edited by I. J. Gruverman (Plenum Press, Inc. New York, 1968), Vol. 4, P. 13-35.

[29] G. Kornfeld, Phys. Rev. **177**, 494 (1969).

[30] C. L. Chien, J. C. Walker, Phys. Rev. B **13**, 1876 (1976).

[31] A. R. Mkrtchyan, A. R. Arakelyan, G. A. Arutyunyan, and L. A. Kocharyan, Pis'ma Zh. Eksp. Teor. Fiz. Pisma **26**, 599 (1977) [JETP Lett. **26**, 449 (1977).

[32] A. R. Mkrtchyan, G. A. Arutyunyan, A. R. Arakelyan, and R. G. Gabrielyan, Phys. Stat. Sol. b **92**, 23 (1979).

[33] S. L. Popov, G. V. Smirnov, and Yu. V. Shvyd'ko, JETP Lett. **49**, 747 (1989).

[34] Yu. V. Shvyd'ko and G. V. Smirnov, J. Phys.: Condens. Matter **4**, 2663 (1992).

[35] A. Abragam, Compt. Rend. **250**, 4334 (1960).

[36] F. J. Lynch, R. E. Holland, and M. Hamermesh, Phys. Rev. **120**, 513 (1960).

[37] L. T. Tsankov, J. Phys. A: Math. Gen. **14**, 275 (1981).

[38] P. Helisto, E. Ikonen, and T. Katila, Hyperfine Interactions **29**, 1563 (1986).

[39] R. N. Shakhmuratov and A. Szabo, Phys. Rev. A **58**, 3099 (1998).

[40] https://www.alfa.com/en/catalog/041580/

[41] https://www.webelements.com/iron/isotopes.html

[42] P. Gütlich, E. Bill, A. X. Trautwein, *Mössbauer Speectroscopy and Transition Metal Chemistry: Fundamentals and Applications* (Springer-Verlag, Berlin, Heidelberg, 2011).

[43] S. Margulies, J. R. Ehrman, Nucl. Instrum. Methods **12**, 131 (1961).